International Journal of Materials Engineering and Technology
© 2017 Pushpa Publishing House, Allahabad, India
http://www.pphmj.com
http://dx.doi.org/10.17654/MT016120041
Volume 16, Numbers 1-2, 2017, Pages 41-52 **ISSN: 0975-0444**

SYNTHESIS AND CHARACTERIZATION OF HEMATITE OBTAINED ON THERMAL DECOMPOSITION OF ACETYL FERROCENE

B. Das[1], J. Kusz[2], V. Raghavendra Reddy[3], M. Zubko[4] and A. Bhattacharjee[1,*]

[1]Department of Physics
Visva-Bharati University
Santiniketan, India

[2]Department of Physics
University of Silesia
Katowice, Poland

[3]UGC-DAE Consortium for Scientific Research
Indore, India

[4]Institute of Materials Science
University of Silesia
Chorzów, Poland

Abstract

Thermal decomposition of acetyl ferrocene was carried out at ~1000°C in a furnace in ambient conditions. The residual product obtained was ~14% by weight. Morphology of the residual material was obtained by scanning electron microscopy. Standard physical characterization

Received: June 10, 2017; Revised: July 11, 2017; Accepted: July 21, 2017
Keywords and phrases: acetyl ferrocene, thermal decomposition, characterization, hematite.
*Corresponding author

techniques like powder XRD, electrical conductivity study, dc magnetization study as well as ^{57}Fe Mössbauer spectroscopy were employed to characterize the thermal decomposition product. The results obtained from those studies unequivocally established that the residual material obtained is hematite. A solid state reaction has been proposed.

1. Introduction

Thermal decomposition of a suitable precursor in solid state represents a very simple way of solventless synthesis towards a desired material. Thermal decomposition method has some definite advantages like its simplicity, low cost and easiness to obtain high purity product. So it is quite promising and facile to be applied into material industry. In case of thermal decomposition process for preparing metal oxide(s), preference is generally given to precursor compounds that decompose at lower temperatures to minimize sintering of the resulting oxide and have minimum interfering side reactions or by-products (volatile compounds) (Rao et al. [18]). Thermal decomposition of iron-bearing precursors is a very popular way to produce iron oxides of different phases (Harmankova et al. [9], Zhang et al. [23], Bhattacharjee et al. [3], Pinna et al. [15], Roy et al. [21] and Parola et al. [14]). Synthesis of magnetic oxides by thermal decomposition of organo-iron compounds has several advantages such as a relatively low temperature of formation of magnetic oxides, a short reaction time and a possibility of using inexpensive iron-organic compounds. The properties of the end decomposition product depend on the chemical nature of the precursor used, temperature and reaction atmosphere. Thermal decomposition of organo-iron precursors has been demonstrated to be very successful in the preparation of iron oxide nanoparticles with controllable size and high quality. In recent times, among the iron-containing organic precursor, the metallocene compound-ferrocene $(C_5H_5)_2Fe$ has become an important material for preparing iron oxide nanostructures through thermal decomposition, e.g., magnetic micro/nanoparticles (Parola et al. [14], Koprinarov et al. [11], Amara et al. [1], Bhattacharjee et al. [4] and Rooj et al. [20]) and nanocomposites (Prakash et al. [16]). In this light, in the present paper,

we demonstrate thermal decomposition of precursor acetyl ferrocene. The thermally synthesized material was characterized by powder XRD, scanning electron microscopy, electrical conductivity study, magnetometry and ^{57}Fe Mössbauer spectroscopy.

2. Experimental Procedures

High quality polycrystalline organometallic compound acetyl ferrocene, $[(C_5H_4COCH_3)Fe(C_5H_5)]$ (AFc in short) was obtained from Strem Chemicals and was used for thermal decomposition without further purification. Thermal decomposition of AFc was studied with the help of thermogravimetry (TG) at 15K/min heating rate. From the TG profile, it was found that AFc undergoes thermal decomposition in multi-steps and completes the thermal decomposition with residual mass of ~14%. With this knowledge, certain amount of AFc in a porcelain boat was placed in a furnace at ~1000°C for 4 hours in ambient atmosphere. After cooling down, the material was collected at room temperature. Thermally decomposed material of AFc thus obtained will be hereafter denoted as AFcD.

The material AFcD was then used for several physical characterizations. X-ray powder diffraction was performed with PAN analytical Emperian powder diffractometer equipped with PIXcell^{3D} detector and a Cu-K_α radiation source. Scanning electron microscopy (SEM) images of AFcD were obtained using Carl Zeiss made EVO 18 Special Edition Scanning Electron Microscope. The dc electrical current through the sample cells of AFcD was measured as a function of temperature using the conventional sandwich cell technique in order to find the activation energy of electrical conduction using sandwich cell technique (Bhattacharjee et al. [3]). Temperature dependence of magnetization in AFcD was measured with SQUID magnetometer. ^{57}Fe Mössbauer spectrum of AFcD was recorded at room temperature using a conventional constant-acceleration spectrometer. The hyperfine parameters were obtained by least squares fitting of the experimental spectra to Lorentzian lines using the Normos Mössbauer software analysis program.

3. Results and Discussion

X-ray powder diffraction (XRD) pattern of AFcD was obtained using Cu-K_α radiation within the range $10^\circ < 2\theta < 150^\circ$. Figure 1 shows the XRD pattern with Rietveld refinement results for AFcD sample for selected 2θ ranges. The observed pattern could be well fitted with two different structures. From the intensity distribution, it is found that the powder pattern gives rise to two components only - one component corresponds to 93.1% of the total intensity while the remaining 6.9% of intensity corresponds to the other component. The XRD pattern of the larger component of AFcD clearly exhibits that most of the diffraction peaks correspond to hematite (JCPDF no. 24-72) and the corresponding lattice parameters estimated are as follows: $a = b = 5.0344(1)$ Å; $c = 13.7457(1)$ Å; $\alpha = \beta = 90.00^\circ$, $\gamma = 120.00^\circ$. From the XRD, peak broadening the mean crystallite size (D) was estimated to be $D = 1091(2)$ Å using the full pattern method implemented in the FullProf program (Rodriguez-Carvajal [19]) on the basis of Scherer formula (Cullity [7]).

In order to find the origin of the other minor component observed in the powder XRD pattern, we suspect any possible contamination of AFcD from the sample container used for thermal decomposition. So, we have carried out separate EDX and XRD studies of the powders obtained by crushing the sample container. Combining the results of both the studies, the composition of the sample container can be best understood as the mixture of the following components: (i) aluminum oxide, Al_2O_3; JCPDF: 01-073-1512; (ii) calcium magnesium carbon oxide, $CaMg(CO_3)_2$; JCPDF: 04-008-8066; (iii) potassium hydrogen sulfide, K(HS); JCPDF: 01-085-0725; (iv) silicon, Si; JCPDF: 01-070-8272; and (v) copper iron sulfide, $CuFeS_2$, JCPDF: 01-073-6353. With this information in hand, when the minor component of the powder XRD pattern of AFcD is analysed, it corresponds to a material isostructural to sodium sulphate which is an incidental matching. In any case, from the complete powder XRD analysis of AFcD, it is found that AFcD

contains 93.1% hematite whereas the remaining are the impurities owing to the contamination due to the sample holder. This contamination might have originated by the unexpected corrosion of the inner surface of the sample container during thermal decomposition of the sample at high temperature. Small amount of impurity has also been detected in Mössbauer studies discussed later.

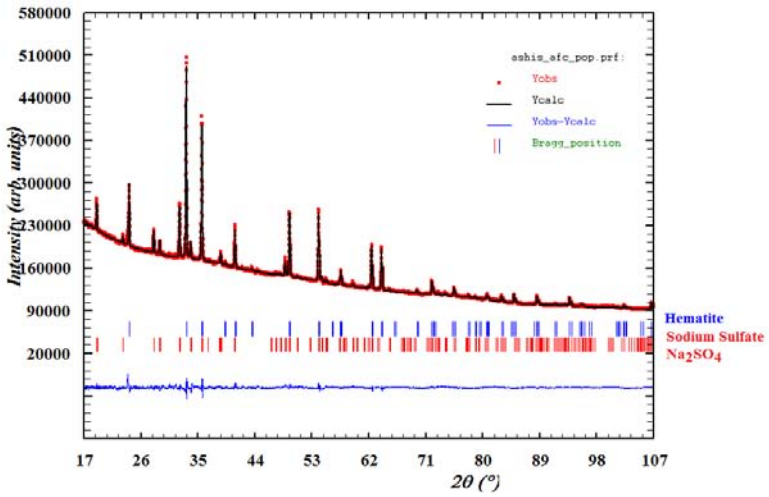

Figure 1. Powder XRD patterns of the decomposed material AFcD at room temperature.

The shape and size of AFcD was studied by SEM. Figure 2 represents the SEM picture of AFcD. From this image, it is clear that the decomposed material is the agglomeration of particles of various shapes and sizes; however, the particles are mostly round-shaped. There are several particles detected with size much lower than 100nm as demonstrated in Figure 2.

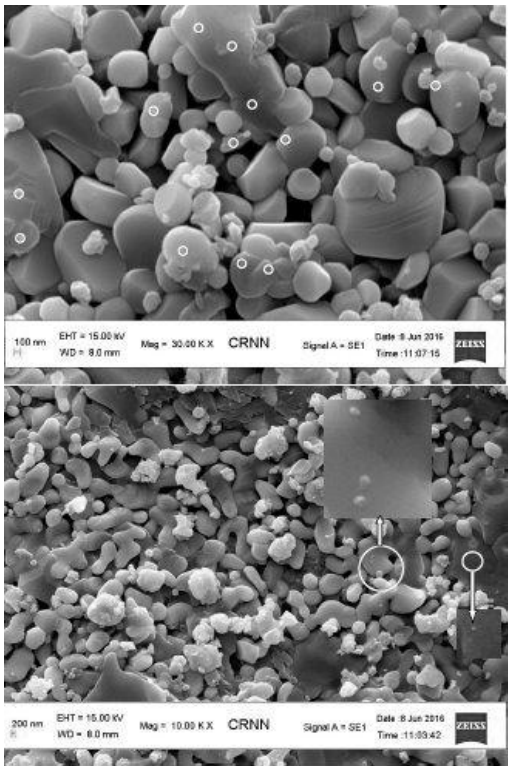

Figure 2. SEM micrographs of the decomposed material of AFcD. Tiny circles on the image are used to visualize the few particles having size much less than 100nm. Inserts show the magnified images of the tiny particles.

Experimentally measured electrical current I passing through the sample cell of AFcD at any absolute temperature T can be expressed by the following Arrhenius relation used for semiconductors (Bhattacharjee et al. [3] and Kao and Hwang [10]):

$$I = I_0 \exp(-E/kT), \tag{1}$$

I_0 being the pre-exponential factor which decides the charge carrier mobility and density of states, E is the electrical activation energy and k is the Boltzmann constant. In the low voltage (Ohmic) region, the steady state current flowing in a semiconductor arises due to the drift of the thermal charge carriers present in the material. The log I vs. $1/T$ plot for AFcD

sample obtained in the Ohmic region (applied voltage = 10V) is shown in Figure 3. The activation energy E obtained from the slope of the plot following equation (1) is 0.42eV. The estimated activation energy value indicates that the decomposed material of AFc is hematite while compared with the reported values of activation energy in the literature (Nikolic et al. [13], Guskos et al. [8] and Cornell [6]).

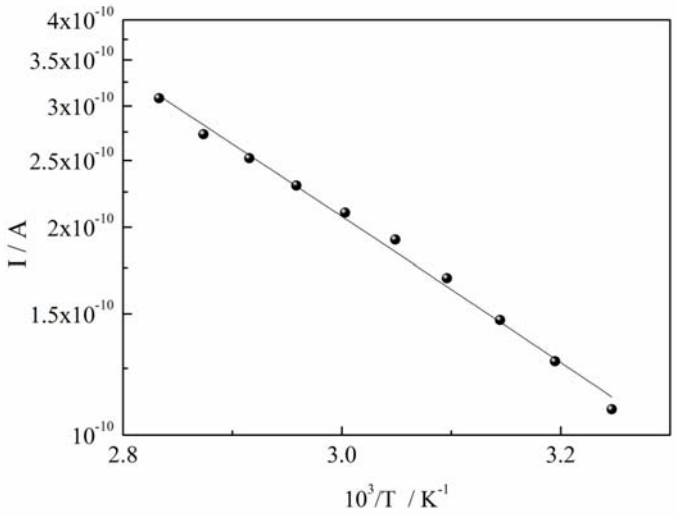

Figure 3. Temperature dependence of the electrical current (I) passing through the sample cell of AFcD.

The temperature (T) dependence of magnetization (M) of AFcD was obtained during thermal cooling-heating cycle in 300-10-300K temperature region under 1kOe magnetic field (Figure 4). The $M(T)$ plot observed during cooling down from room temperature shows a sharp drop in magnetization values at 264K which continues till ~200K. Below this temperature, the $M(T)$ values increase very slowly till the lowest measured temperature (10K). While heating above 10K, the $M(T)$ plot retraces the same path as seen upon cooling till 200K. Beyond this temperature, the $M(T)$ values rapidly increase and ultimately meet the cooling profile at higher temperatures and then very slowly increase with temperature. Thus, a

thermal hysteresis loop of ~6K width in the $M(T)$ plot, associated with a sharp change in $M(T)$ values and centered around 250K, is observed. It is well known that a magnetic phase transition from a weakly ferromagnetic to an antiferromagnetic state occurs in hematite on cooling below the Morin temperature $(T_M = 260\text{K})$ (Zysler et al. [25]) during which the antiferromagnetic ordering is reorganized from being aligned perpendicular to the *c*-axis (above T_M) to be aligned parallel to the *c*-axis below T_M. Morin transition is a yardstick for hematite (α-Fe_2O_3) materials (Zhao et al. [24]). The observed $M(T)$ plots for AFcD with a thermal hysteresis within 200-264K as illustrated in Figure 4 correspond to the Morin transition occurring in the presently obtained decomposed material of AFc which confirms that the decomposed material is hematite.

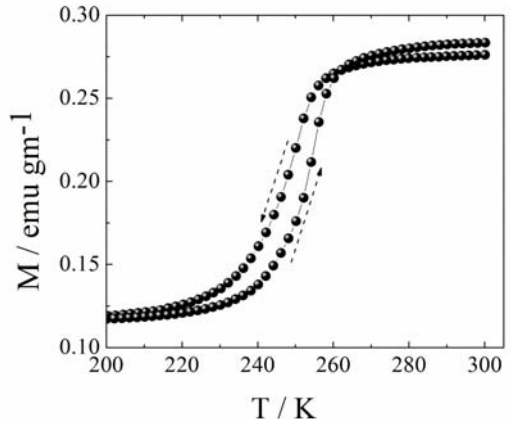

Figure 4. Temperature dependence of magnetization of AFcD under 1kOe magnetic field. Arrows are guide to the eyes.

^{57}Fe Mössbauer spectrum of AFcD was recorded under zero applied magnetic field at 300K (Figure 5). The experimental spectrum could be well fitted with a single sextet with the isomer shift (δ) with respect to α-iron, quadrupole splitting (ΔE_s), hyperfine field (B_{hf}) and the line width as the adjustable parameters for the spectral fits. The sextet observed at 300K indicates the presence of long-range magnetic order in this material at this

temperature. The hyperfine parameters $\delta, \Delta E_s$ and B_{hf} were estimated from the best-fitted spectra and the corresponding values obtained are $0.40 \pm 0.06 \text{mm/s}, \; -0.18 \pm 0.01 \text{mm/s}, \; 50.12 \pm 0.03$ Tesla. The observed hyperfine parameters for iron in AFcD estimated at 300K are in good agreement with those of hematite (Bhattacharjee et al. [4], Rooj et al. [20] and Lyubutin et al. [12]). For better fitting of the observed Mössbauer data, a small doublet has been incorporated and this may be due to impurities. Thus, from the present Mössbauer spectroscopic study, it is established that the thermally decomposed material obtained from AFc is of hematite phase and is in complete agreement with the observations made from the electrical conductivity and magnetic studies.

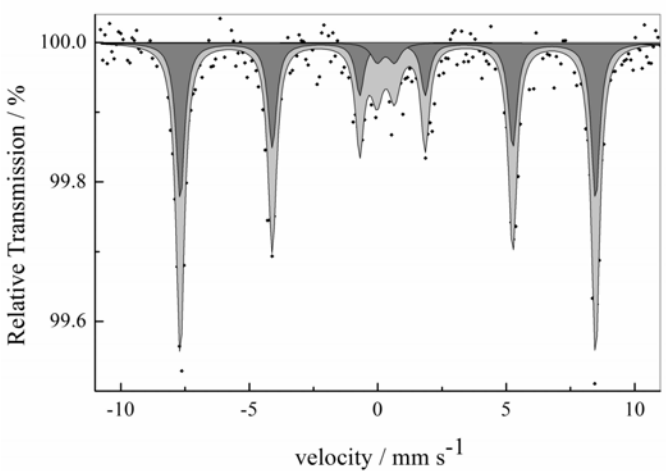

Figure 5. ^{57}Fe Mössbauer spectrum of AFcD obtained at 300K.

The results obtained so far in the present study demonstrate that the thermal decomposition reaction of acetyl ferrocene leads to hematite. It is reported that AFc when thermally decomposed in presence of β-cyclodextrin gives rise to hematite (Yilmaz et al. [22]). There are several reports on the formation of hematite having various shapes or sizes through thermal decomposition of ferrocene mentioned in Introduction. Acetyl ferrocene is solid at room temperature and unlike ferrocene which sublimates at 448K, it boils at ~355K and then thermally decomposes in different steps and results

ultimately in hematite. The solid state reaction based on literature may be understood in the following way. During heating, AFc may give rise to CO/CO_2, CH_4 and C_5H_6 gases (Parola et al. [14]). CO_2/CO, thus, produced may be deoxidized to oxygen and carbon by metallic iron liberated from the thermal decomposition of acetyl ferrocene like ferrocene (Qian et al. [17]) and/or due to reduction of acetyl ferrocene to metallic iron. The metallic iron then may react with available oxygen giving rise to α-Fe_2O_3 (hematite) (Angermann and Töffer [2]). The oxidation of acetyl ferrocene by available atmospheric oxygen in the reaction environment though small in amount, may be an additional reaction mechanism forming hematite nanoparticles. As no traceable C is observed in the residual product and the observed Mössbauer spectra of the studied samples do not exhibit any trace of iron carbide (Fe_3C) or free iron (Fe), it is quite likely that C is an intermediate product which might have been oxidized to CO_2/CO. Thus, the proposed reaction may lead to the formation of hematite as only solid residual product of thermal decomposition while others being volatile. Thermogravimetry (TG) is a technique which provides the profile of mass loss with increasing temperature during a solid state reaction, while an evolved gas analyzer (EGA) provides the information on the different gaseous products formed during the solid state reaction. Thus, the solid state reaction proposed above can be confirmed by a thermogravimetry study with simultaneous evolved gas analysis which is drawing our present interest.

4. Conclusion

Thermal decomposition study of an organometallic compound acetyl ferrocene has been carried out. The decomposed material has been characterized by different conventional physical characterization techniques. The observed results have undoubtedly confirmed that the material, thus, obtained is hematite. The present manuscript describes a simple process for the preparation of hematite particles by solventless thermal decomposition of acetyl ferrocene. Studies are in progress to explore the effect of reaction promoters and ambience on the thermal decomposition of acetyl ferrocene in order to have further control on the size of the particles, thus, produced.

Thermal decomposition of organometallic precursors leading to iron oxide nanoparticles of controllable size/shape with no interfering solid by-products is an explorable research area.

Acknowledgements

Financial support for the thermogravimetry analyzer (STA 449 F3 Jupiter) from the Department of Science and Technology (DST), Govt. of India through FIST-2010 to the Department of Physics is gratefully acknowledged. Mössbauer spectroscopic studies were carried out using the facilities of UGC-DAE CSR at Indore Center for which the author A. Bhattacharjee is thankful to that authority.

References

[1] D. Amara, J. Grinblat and S. Marge, J. Mater. Chem. 22 (2012), 2188.

[2] A. Angermann and J. Töffer, J. Mater. Sci. 43 (2008), 5123.

[3] A. Bhattacharjee, D. Bhakat, M. Roy and J. Kusz, Physica B 405 (2010), 1546.

[4] A. Bhattacharjee, A. Rooj, M. Roy, J. Kusz and P. Gütlich, J. Mater. Sci. 48 (2013), 2961.

[5] A. Bhattacharjee, D. Roy, M. Roy, S. Chakraborty, A. De, J. Kusz and W. Hofmeister, J. Alloys Compd. 503 (2010), 449.

[6] R. M. Cornell and U. Schwertmann, The Iron Oxides, Weinheim, NewYork, 1996.

[7] B. D. Cullity, Elements of X-ray Diffraction Reading, Addison-Wesley, 1956, p. 531.

[8] N. Guskos, G. J. Papadopoulos, V. Likodimos, S. Patapis, D. Yarmis, A. Przepiera, K. Przepiera, J. Majszczyk, J. Typek, M. Wabia, K. Aidinis and Z. Drazek, Mater. Res. Bull. 37 (2002), 1051.

[9] P. Harmankova, M. Hermanek and R. Zboril, Eur. J. Inorg. Chem. 2010 (2010), 1110.

[10] K. C. Kao and W. Hwang, Electrical Transport in Solids, Pergamon Press, NY, 1981.

[11] N. Koprinarov, M. Konstantinova and M. Marinov, Solid State Phenomena 159 (2010), 105.

[12] I. S. Lyubutin, C. R. Lin, Y. V. Korzhetskiy, T. V. Dmitrieva and R. K. Chiang, J. Appl. Phys. 106 (2009), 34311.

[13] M. V. Nikolic, M. P. Slankamenac, N. Nikolic, D. L. Sekulic, O. S. Aleksic, M. Mitric, T. Ivetic, V. B. Pavlovic and P. M. Nikolic, Science of Sintering 44 (2012), 307.

[14] S. Parola, R. Papiernik, L. G. Hubert-Pfalzgraf, S. Jagner and M. Hkansson, J. Anal. Appl. Pyrol. 120 (2016), 399.

[15] N. Pinna, G. Garnweitner, M. Antonietti and M. Niederberger, J. Am. Chem. Soc. 127 (2005), 5608.

[16] R. Prakash, A. K. Mishra, A. Roth, C. Kübel, T. Scherer, M. Ghafari, H. Hahn and M. Fichtner, J. Mater. Chem. 20 (2010), 1871.

[17] W. Qian, Q. Chen, F. Cao and C. Chen, Open. Mater. Sci. J. 2 (2008), 19.

[18] C. N. R. Rao, M. Muller, A. K. Cheetham, eds., The Chemistry of Nanomaterials: Synthesis, Properties, Applications, Wiley-VCH, Weinheim, 2004.

[19] J. Rodriguez-Carvajal, Physic B 192 (1993), 55.

[20] A. Rooj, M. Roy, J. Kusz and A. Bhattacharjee, Int. J. Exp. Spect. Tech. 1 (2016), 003.

[21] D. Roy, M. Roy, M. Zubko, J. Kusz and A. Bhattacharjee, Int. J. Thermophysics 37 (2016), 93.

[22] V. T. Yilmaz, A. Karadag and H. Icbudak, Thermochim. Acta. 261 (1995), 107.

[23] Y. C. Zhang, J. Y. Tang and X. Y. Hu, J. Alloys Compd. 462 (2008), 24.

[24] B. Zhao, Y. Wang, H. Guo, J. Wang, Y. He, Z. Jiao and M. Wu, Mater. Sc. Poland 25 (2007), 1143.

[25] R. D. Zysler, D. Fiorani, A. M. Testa, M. Godinho, E. Agostinelli and L. Suber, J. Magn. Magn. Mater. 272 (2004), 1575.